IEEE Access
SPECIAL SECTION ON DATA-ENABLED INTELLIGENCE FOR DIGITAL HEALTH

Received June 17, 2019, accepted June 30, 2019, date of publication July 3, 2019, date of current version July 31, 2019.

Digital Object Identifier 10.1109/ACCESS.2019.2926523

Automatic Detection Approach for Bioresorbable Vascular Scaffolds Using a U-Shaped Convolutional Neural Network

WEN ZHOU[1,2], (Member, IEEE), FEI CHEN[3], YONGSHUO ZONG[4], DADONG ZHAO[1], BIAO JIE[1,2], ZHENGDONG WANG[1], CHENXI HUANG[4], AND EDDIE Y. K. NG[5]

[1]School of Computer and Information, Anhui Normal University, Wuhu 241002, China
[2]Anhui Provincial Key Laboratory of Network and Information Security, Wuhu 241002, China
[3]Department of Cardiology, Shanghai Tongji Hospital, Tongji University, Shanghai 200092, China
[4]Department of Computer Science, Tongji University, Shanghai 201804, China
[5]School of Mechanical and Aerospace Engineering, Nanyang Technological University, Singapore 639798

Corresponding authors: Wen Zhou (w.zhou@ahnu.edu.cn) and Fei Chen (riverapt@126.com)

This work was supported in part by the National Natural Science Foundation (NSFC) of China under Grant 61573023, and in part by the Doctoral Scientific Research Foundation of Anhui Normal University.

ABSTRACT Artificial stent implantation is one of the most effective ways to treat vascular diseases. However, commonly used metal stents have many negative effects, such as being difficult to remove and recover, whereas bio-absorbable stents have become the best way to treat vascular diseases because of their absorbability and harmlessness. It is very important in vascular medical imaging, such as optical coherence tomography (OCT), to be able to effectively track the position of stents in blood vessels. This task is undoubtedly labor-intensive, and it is inefficient to rely on experts to identify various scaffolds from medical images. In this paper, a novel automatic detection method for bioresorbable vascular scaffolds (BVSs) via a U-shaped convolutional neural network is developed. The method is composed of three steps: data preparation, network training, and network testing. First, in the data preparation step, we complete the task of labeling related samples based on expert experience, and then, these labeled OCT images are divided into the original and masked OCT images (corresponding to X and Y in supervised learning, respectively). Next, we train our data on a U-shaped convolutional neural network, which consists of five downsampling modules and four upsampling modules. We can obtain a related training model, which can be used to predict the related samples. In the testing stage, we can easily utilize the trained model to predict the input OCT data so that we can obtain the relevant information about a BVS in an OCT image. Obviously, this method can assist doctors in diagnosing the disease and in making important decisions. Finally, some experiments are performed to validate our proposed method, and the IoU criterion is used to measure the superiority of our proposed method. The results show that our proposed method is completely feasible and superior.

INDEX TERMS Stent implantation, vascular disease, optical coherence tomography, bioresorbable vascular scaffolds, U-shape.

I. INTRODUCTION

Recently, bioresorbable vascular scaffolds (BVSs) have been adopted in some coronary artery treatment regimes as the latest stent type. In particular, they are currently the only type approved by the Food and Drug Administration. However, how to detect the position of BVS in a biomedical image is always a difficult task. Traditionally, such a detection task mainly depends on experts in artery treatment, but such manual detection is very time consuming and labor intensive. In fact, the scale of biomedical images is very large, and a pullback sequence of vascular imaging always consists of dozens of images; therefore, to some extent, it is not effective to use experts to manually detect stents. On the other hand, deep learning methods have greatly progressed in the past 3 years, and many novel network structures and methods have been proposed by dozens of scholars and researchers. In fact, deep learning methods have been increasingly employed to

The associate editor coordinating the review of this manuscript and approving it for publication was Ying Song.

solve biomedical problems, for instance, in the detection of organ tissues, object acquisition and recognition, and assistance in surgery.

In fact, for a vascular stenting surgery, it is very important to determine whether the position of the implanted stent is close to a vessel wall and, to some extent, to determine whether the surgery is successful. In this paper, we conduct a related task to attempt to solve the position dilemma of BVSs. We propose a novel pipeline to detect BVSs, consisting of two parts: data preprocessing and network training. We employ the U-shaped network to detect BVSs.

The contribution of our proposed approach is mainly as follows:

1) We employ several vascular stenting experts to conduct the related tagging job for BVC OCT images and to build the related BVC OCT dataset. We split the whole dataset into two parts according to the labels. In this way, we can use supervised learning to train our network.
2) We improve the whole structure of the U-shaped network to be better suited to train biomedical OCT images.

The remainder of the paper is organized as follows. In Section II, we briefly review the related work on vascular stents and neural networks. In Section III, we show our proposed approach. Section IV shows the related algorithms. Section V shows the results of our experiments. Finally, in Section VI, we draw our conclusions.

II. RELATED WORKS

Many hundreds of thousands of stents have been implanted. Intravascular optical coherence tomography (OCT) is an important, emerging imaging technique. However, it may take 16 hours or more to manually analyze hundreds of images and thousands of stent struts from a single pullback. To solve this kind of time-consuming and labor-extensive problem, many scholars have proposed many different methods.

Wang *et al.* [1] proposed a novel method based on a Bayesian network and graph searching. In detail, they completed a study stage via a Bayesian network, and then a graph search was performed on enface projections using minimum spanning tree algorithms. The depths of all struts in a pullback were simultaneously determined using the graph cut method. However, this method is only suitable for OCT images of metallic stent struts, rather than OCT images of bioresorbable vascular scaffolds (BVSs). In addition, several studies on metallic stent detection in OCT images have been published [2]–[8]. Specifically, Xu *et al.* [2] proposed a 2D ridge detector, and they focused on a restricted category of cases in which stents appeared as elongated ridges due to very thick tissue coverage. In [4], Tsantis et al. applied probabilistic neural networks to detect stent struts based on many struts features extracted using continuous wavelet filters. However, because this method used images obtained from femoral arteries, the performance of this approach in clinical intra-coronary OCT images may be unknown. Additionally, Lu *et al.* [5] adopted bagging decision trees as the classifier for an initial screen of candidate struts and achieved promising results in a moderately sized validation dataset. Such classification-based approaches can utilize human expert knowledge and can easily combine multiple features for decision-making and are potentially more robust. In [6], Wang et al. employed a single A-line analysis to capture the signatures of individual scaffolds. Mandelias *et al.* [7] extended the wavelet-based detection method and achieved a higher accuracy and shorter processing time, but the size of the validation data set was small (only 4 pullbacks). Nevertheless, all of these methods used local image features of individual struts for detection without considering the continuity of the cylindrical shape of the scaffolds. In addition, for bioresorbable vascular scaffolds (BVSs), it is difficult to achieve a good performance using these methods because it is more difficult to extract and describe the features of OCT images of BVSs than those of metallic stents. Previously, there exist few studies on automatic BVS analysis (including detection); Wang *et al.* [9] presented a greyscale-based method, which extracted the grey and gradient features and employed many different thresholds to directly segment the BVS struts. In particular, this method can hardly be generalized because the intensity and contrast vary across images. Lu *et al.* [10] proposed a two-step framework for a scaffold analysis: using an AdaBoost detector for strut detection and employing dynamic programming for strut segmentation. However, while struts are structurally incomplete or under several blood artifacts, the detection performance is often poor and thus makes the subsequent segmentation and malapposition analysis inaccurate. In addition, Huang *et al.* [11] also presented a detection method for BVS in IOCT based on region growing. However, to obtain a good performance, this method requires many samples or pullbacks, and the requirements for quality in IOCT are high.

In recent years, a deep learning framework has achieved excellent results in the computer visual object detection and recognition domain [12], and it has attracted increasing attention and led to research or studies based on this framework. Unlike traditional machine learning methods that depend on manually designed features, in deep learning approaches, novel representation patterns or models are automatically learned from low-level features to high-level semantics, which often makes the detection performance more correct and robust. Cao *et al.* [15] proposed a deep learning-based detection method for BVS struts in IOCT images; it uses the R-CNN framework [13], [14], which is another famous framework in deep learning, to achieve the representation of the features. In addition, a prevalent network family in deep learning, known as a U-shaped convolutional neural network (U-Net) [16], has achieved significantly excellent performance gains in object segmentation and recognition. U-Net studies object features by using many convolutional neural networks during training and employing them for detection afterwards. In this paper, we attempt to use U-Net to achieve the detection and segmentation task of BVS struts.

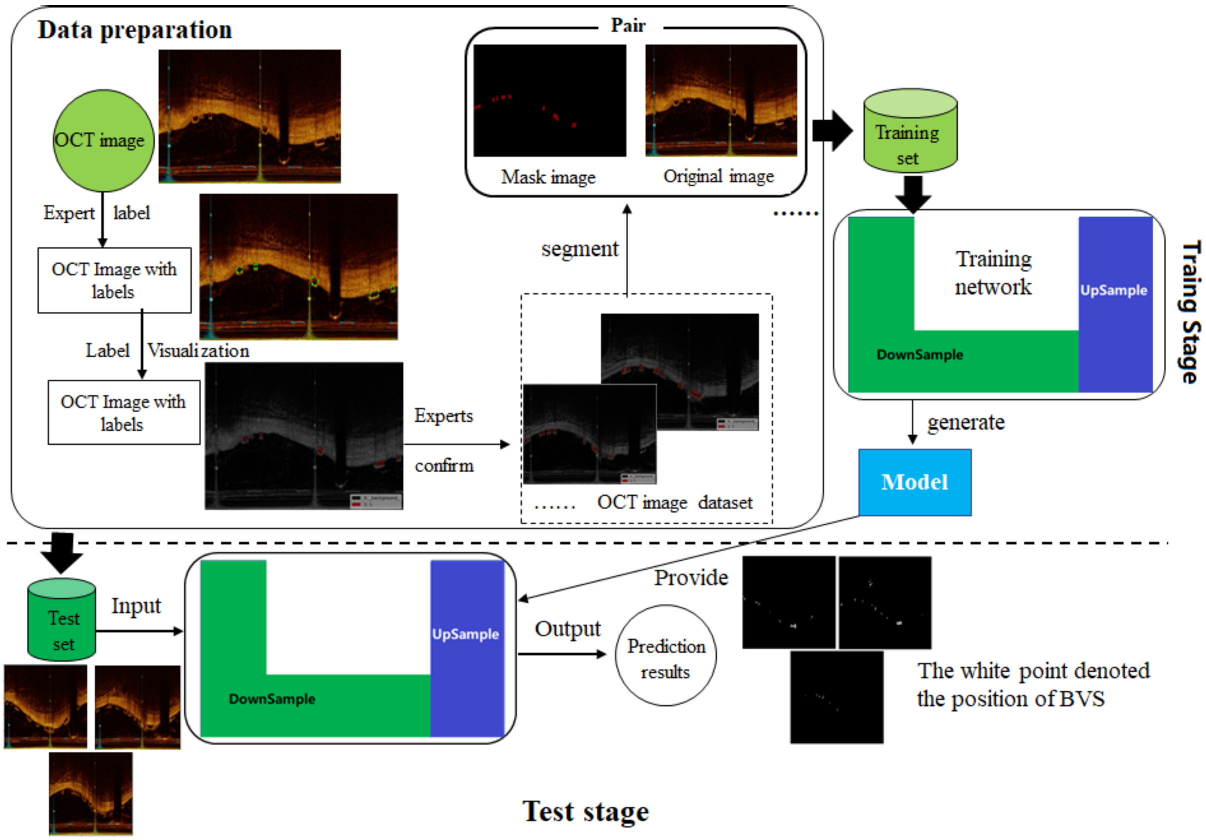

FIGURE 1. The overview of our proposed method.

Compared with the method proposed in [15], our proposed method does not require two steps to complete the segmentation task; additionally, our proposed method consumes less time than the method proposed in [15], while excellent results are capable of being achieved. If any segmentation task is able to effectively finish, it must be assured that the target object has been completely and accurately detected.

III. OVERVIEW OF PROPOSED APPROACH

In this section, the overview of the proposed approach is shown. Our approach comprises three parts, i.e., data preparation, data training and data testing. The main structure of the proposed method is as follows (**Figure 1**).

Data preparation is an important step and is the foundation of the following steps. In the training step, by better and completely achieving the relevant training task, we can provide training model data to predict the input OCT image in the testing stage. In the testing stage, the prediction result can be obtained to help doctors diagnose the disease or decide whether vascular surgery was successful.

In the following section, the details of the proposed method are shown.

IV. DETAILS OF THE PROPOSED METHOD

A. DATA PREPARATION

The flow of data preparation is shown in **Figure 2**. We obtain relevant IOC BVS images from eight pullbacks. Then, we ask experts to label these BVS images. In this paper, the LabelMe tool is used to tag the related BVS positions. In fact, it is very hard for full labeling to completely identify a BVS position using a serials of polygons, even for a very professional expert. The reason is obvious: every piece of the BVS image describes only a viewpoint of the OCT pullback; therefore, some BVSs may be obscured by some obstacles, such as vessel walls. In particular, the labeling polygon only abstractly represents the closest position of a BVS.

After the experts complete the labeling task for every OCT image, the labeled data are shown to experts to further confirm the final result. In this step, an expert can modify their labeling result to optimize the final result. If the expert finds some incorrect labeling information, a related revision task will be performed. The purpose of the above jobs is to enhance the quality of the samples.

Furthermore, a segmentation job is conducted to obtain the relevant masked OCT images. Masked OCT images are black-white images, for which the white pixels denote the BVS information. More specifically, a pixel-to-pixel operation can be used to handle these masked images to restore the labeling information to the OCT image.

Last, but not least, we can obtain the related training and test datasets, which are divided into two different datasets according to a 70:30 ratio, respectively.

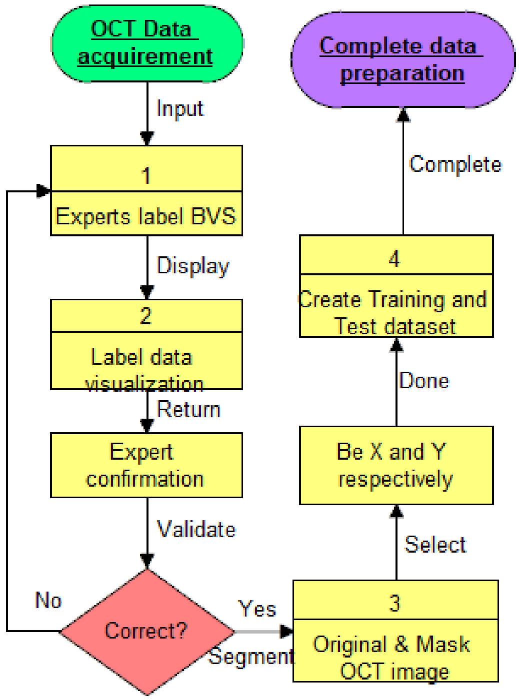

FIGURE 2. The flow of the OCT image preparation. The main steps comprise four steps: Labeling by experts, data label visualization, segment-labeling OCT images and creating the training and test datasets.

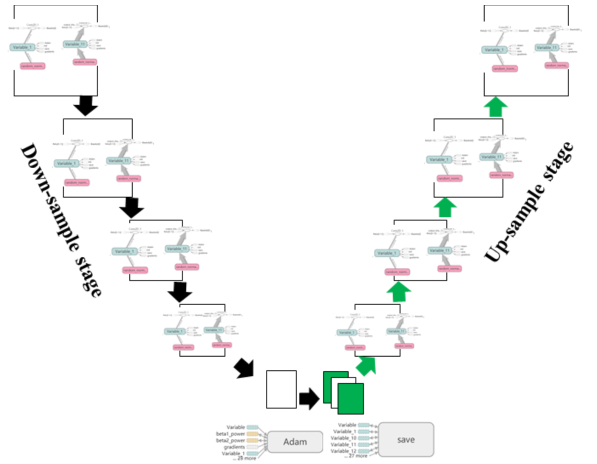

FIGURE 3. The structure of the proposed U-shaped network, which consists of five downsampling modules and four upsampling modules.

TABLE 1. The detailed parameter information of the proposed U-shaped network.

Layer	Attribute	Weights	Biases	Purpose
DS1	Conv	[3,3,3,64]	[64]	Downsampling
DS1	Conv	[3,3,64,64]	[64]	Downsampling
DS1	MaxPooling	[1,2,2,1]	-	-
DS2	Conv	[3,3,64,128]	[128]	Downsampling
DS2	Conv	[3,3,128,128]	[128]	Downsampling
DS2	MaxPooling	[1,2,2,1]	-	-
DS3	Conv	[3,3,128,256]	[256]	Downsampling
DS3	Conv	[3,3,256,256]	[256]	Downsampling
DS3	MaxPooling	[1,2,2,1]	-	-
DS4	Conv	[3,3,256,512]	[512]	Downsampling
DS4	Conv	[3,3,512,512]	[512]	Downsampling
DS4	MaxPooling	[1,2,2,1]	-	-
DS5	Conv	[3,3,512,1024]	[1024]	Downsampling
DS5	Conv	[3,3,1024,1024]	[1024]	Downsampling
DS5	MaxPooling	[1,2,2,1]	-	-
US1	Conv-Transpose	[3,3,1024,1024]	[1024]	Upsampling
US2	Conv-Transpose	[3,3,512,1O24]	[512]	Upsampling
US3	Conv-Transpose	[3,3,256,512]	[256]	Upsampling
US4	Conv-Transpose	[3,3,128,256]	[128]	Upsampling
Out	Conv	[1,1,128,1]	[1]	Output

B. U-SHAPED NETWORK

In essence, the U-shaped network is a two-stage network. The first stage performs a downsampling task, and the second stage conducts an upsampling job. In particular, the downsampling module is composed of two convolutional operations and one max pooling operation. The parameter information can be seen in Table 1.

In addition, the structure of the proposed U-shape network is shown in Figure 3. There are five downsampling modules and four upsampling modules. In addition, the upsampling module consists of a convolution transpose operation, and its purpose is to scale up the image by decreasing the quantities of patches obtained by downsampling.

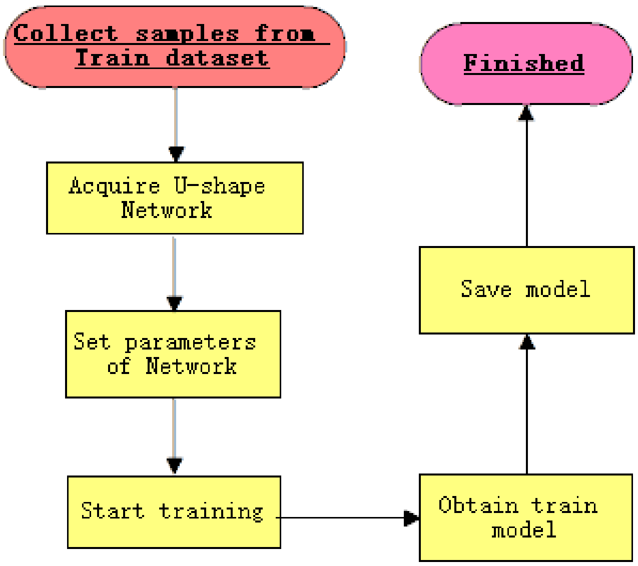

FIGURE 4. The flow of train our OCT data using Proposed U-shape network.

C. TRAINING AND TESTING TASKS

Previously, the data preparation and network acquisition steps were performed; in this section, the training and testing tasks are scheduled to finish the automatic BVS detection job. The basic flow for training the proposed U-shape network is shown in Figure 4. The process of the training network is as follows.

(1) The architecture of the proposed network is obtained; as mentioned above, the network consists of five downsampling modules and four upsampling modules.

(2) Set the parameters of the network to relevant values. Because there does not exist a pre-training model based on the proposed network, intuitively, we adopt a normally distributed random function to initially assign the related parameters. Obviously, it may take more

time to finish the job of training our network. However, the samples are very limited; therefore, very little effect may have been placed on our network.

(3) Start the training task, and save the trained model. Before we start to perform the training job, we must perform some operation to input a uniform OCT image of the same size to the proposed network. Obviously, a larger number of input images would yield better results, but it will be more time consuming. Considering different conditions, in this paper, the sized of the input OCT image is 256 × 256.

V. EXPERIMENTS

In this section, we perform the related experiments to validate the proposed approach.

A. ENVIRONMENT

We implement our proposed approach in Python. Moreover, we use the open source TensorFlow library to complete the network learning job. In addition, the program is executed on a PC under Windows 10 with an Intel Core I7-7700HQ processor with 8 GB of physical memory and an NVIDIA GeForce GTX 1060 GPU with 6 GB of memory.

To train the network, we collected 8 related OCT pullbacks from Tongji Hospital, Shanghai, China. In particular, there are 100 frames for every pullback, and we can obtain an OCT image from every frame of a pullback. Finally, we divide these samples into training and test datasets (i.e., 70% vs. 30%, respectively). Next, the related experimental results are shown to validate our proposed method.

B. TRAINING TASK OF NETWORK

The loss function is an important criterion from which to measure the performance of the training network. In the training stage, we validate the training result after every epoch. In this paper, we use 500 epochs. The comparative results between the training loss and the validation loss can be seen in Figure 5.

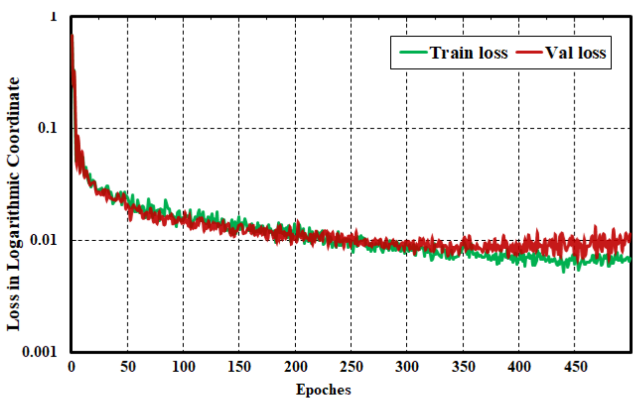

FIGURE 5. Comparison between the training loss and the validation loss on a logarithmic scale.

From Figure5, it is not hard to find that the training loss gradually becomes smaller than the validation loss as the training epoch increases. In fact, for a qualified training model, the value based on the training loss indicator should be better than the value based on the validation loss. In addition, the smaller the difference between the training loss and the validation loss is, the better the performance of training model.

Hence, in the training stage, the trained model is qualified to correctly predict the result.

C. TEST TASK OF NETWORK

Previously, a training model was performed with a related task to measure the performance of the proposed network. The IoU (Intersect of Union) indicator is used to measure the accuracy of the prediction result. The IoU indicator is as follows (equation 1).

$$IoU(P, A) = \sum_{\alpha \in P, \beta \in A} \frac{\Theta(\alpha) \cap \Theta(\beta)}{\Theta(\alpha) \cup \Theta(\beta)} \quad (1)$$

where the terms P and A represent the predicted result and the actual result (ground truth), respectively. In addition, the variable α, β is the BVS in the corresponding OCT image. Additionally, the function Θ is used to compute the area of the relevant BVS. The operations $\cap$ and $\cup$ are the intersect and union operations, respectively, for every BVS between the predicted and the actual masked images.

However, as mentioned above, in performing the labeling task for OCT images, we only approximate the position of BVS using some polygons. More specifically, some mistakes may exist, and it is almost impossible to perfectly label the position of an BVS in an OCT image. Because there are many factors that affect our final labeling result to some extent, such as some obstacles obscure part of the BVS (e.g., vessel walls and blood).

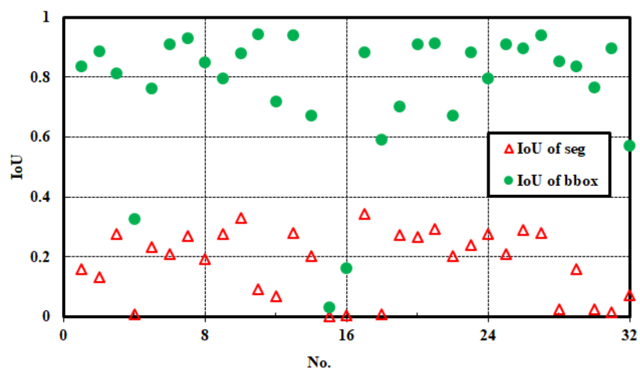

FIGURE 6. Comparison between the IoU of seg and the IoU of the bounding box results.

To better evaluate our proposed method, the bounding box of a BVS is used to evaluate the accuracy of the results. In fact, in the predicted and actual results, for every BVS (i.e., the white points in results), we directly complete the comparative result with the IoU indicator: we called it the IoU of seg (for a masked image, every BVS is seen as a seg). In addition, a bounding box of every seg is performed, which is referred to as the IoU of bbox. The related result can be seen in Figure 6.

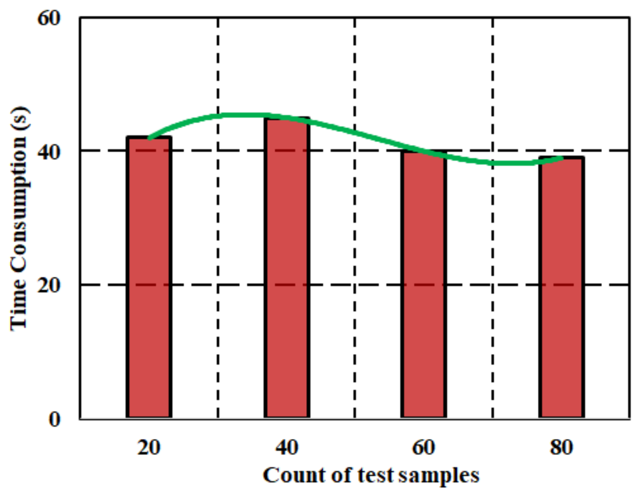

FIGURE 7. Time consumption of the prediction task with different numbers of samples.

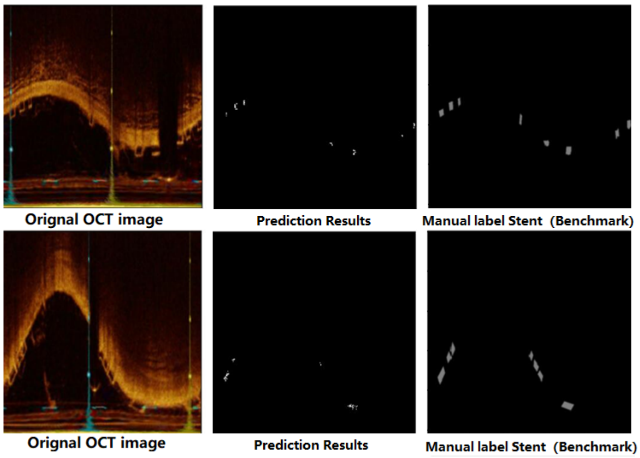

FIGURE 8. Comparison between the predicted and actual results.

From Figure6, it is not hard to find that a better result is that from IoU of bbox. Conversely, the IoU of seg method yields poor results. The explanation of this result is that our prediction result obtained only the approximated position of a BVS, rather than the same position. In practice, the approximated result based on the prediction is enough because the actual position of a BVS is also an approximated representation.

Therefore, the accuracy of the proposed method is completely superior and feasible. That is, the design requirements can be met.

Furthermore, we conducted another experiment to evaluate the computational time of the prediction. Obviously, the time consumption of the prediction is very important; above all, users do not tolerate that relevant predictions that take too long. In general, an expert spends approximately one minute to label fifty OCT images. Therefore, for the same number of images, the prediction time should not be greater than one minute.

The results of time consumption experiment are shown in Figure 7.

In Figure 7, we can see that the time consumption stabilizes as the number of samples increases. Moreover, as the number of samples increases, the time consumption sometimes progressively decreases, and it is always less than one minute. Obviously, the prediction speed is faster than that of an expert, not to mention an ordinary person.

Finally, the test results are shown in Figure 8, and a comparative result is shown in every row. It is not hard see that based on the predicted results of our method, the approximate position of every BVS is almost achieved. Certainly, the predicted size of a BVS is sometimes smaller than the actual (ground truth or benchmark) size because the number of training samples is insufficient.

VI. CONCLUSION

In this paper, we complete the automatic detection of BVSs in OCT images. We propose a novel U-shaped network, with five downsampling modules and four upsampling modules. In addition, to conduct the relevant training and testing jobs, we perform a related data preparation task. Experts labeled the data and segmented the labeled data into the original data and the masked data. The masked data are used as the ground truth to evaluate the predicted result of the network. Additionally, we adopt the IoU indicator to evaluate the accuracy of the proposed method. Furthermore, because the labeling information is abstract and approximated using simply polygons, we utilize the bounding box of the predicted target results to evaluate and achieve better results. Finally, experiments are used to show the superiority and feasibility of the proposed method.

However, our proposed method still need to be improved in order to achieve better results. In the future, we plan to further improve the accuracy of the proposed method. The solutions include adding complexity of the network, enlarging the scale of the training samples, and integrating the proposed method to form an application. In this way, the proposed method can handle actual data and help surgeons and doctors solve some tedious and labor-intensive jobs.

ACKNOWLEDGMENT

The authors appreciate the comments and suggestions from all the anonymous reviewers, whose comments significantly improved this paper.

REFERENCES

[1] Z. Wang, M. W. Jenkins, G. C. Linderman, H. G. Bezerra, Y. Fujino, M. A. Costa, D. L. Wilson, and A. M. Rollins, "3-D stent detection in intravascular OCT using a Bayesian network and graph search," *IEEE Trans. Med. Imag.*, vol. 34, no. 7, pp. 1549–1561, Jul. 2015.

[2] C. Xu, J. M. Schmitt, T. Akasaka, T. Kubo, and K. Huang, "Automatic detection of stent struts with thick neointimal growth in intravascular optical coherence tomography image sequences," *Phys. Med. Biol.*, vol. 56, no. 20, pp. 6665–6675, Sep. 2011.

[3] G. J. Ughi, T. Adriaenssens, K. Onsea, P. Kayaert, C. Dubois, P. Sinnaeve, M. Coosemans, W. Desmet, and J. D'hooge, "Automatic segmentation of in-vivo intra-coronary optical coherence tomography images to assess stent strut apposition and coverage," *Int. J. Cardiovascular Imag.*, vol. 28, no. 2, pp. 229–241, Feb. 2012.

[4] S. Tsantis, G. C. Kagadis, K. Katsanos, D. Karnabatidis, G. Bourantas, and G. C. Nikiforidis, "Automatic vessel lumen segmentation and stent strut detection in intravascular optical coherence tomography," *Med. Phys.*, vol. 39, no. 1, pp. 503–513, Jan. 2012.

[5] H. Lu, M. Gargesha, Z. Wang, D. Chamie, G. F. Attizzani, T. Kanaya, S. Ray, M. A. Costa, A. M. Rollins, H. G. Bezerra, and D. L. Wilson, "Automatic stent detection in intravascular OCT images using bagged decision trees," *Biomed. Opt. Express*, vol. 3, no. 11, pp. 2809–2824, Nov. 2012.

[6] A. Wang, J. Eggermont, N. Dekker, H. M. Garcia-Garcia, R. Pawar, J. H. Reiber, and J. Dijkstra, "Automatic stent strut detection in intravascular optical coherence tomographic pullback runs," *Int. J. Cardiovascular Imag.*, vol. 29, no. 1, pp. 29–38, 2013.

[7] K. Mandelias, S. Tsantis, S. Spiliopoulos, P. F. Katsakiori, D. Karnabatidis, G. C. Nikiforidis, and G. C. Kagadis, "Automatic quantitative analysis of in-stent restenosis using FD-OCT in vivo intra-arterial imaging," *Med. Phys.*, vol. 40, no. 6, 2013, Art. no. 063101.

[8] A. Wang, J. Eggermont, N. Dekker, P. J. D. Koning, J. H. Reiber, and J. Dijkstra, "3D assessment of stent cell size and side branch access in intravascular optical coherence tomographic pullback runs," *Computerized Med. Imag. Graph.*, vol. 38, no. 2, pp. 113–122, 2014.

[9] A. Wang, S. Nakatani, J. Eggermont, Y. Onuma, H. M. Garcia-Garcia, P. W. Serruys, J. H. C. Reiber, and J. Dijkstra, "Automatic detection of bioresorbable vascular scaffold struts in intravascular optical coherence tomography pullback runs," *Biomed. Opt. Express*, vol. 5, no. 10, pp. 3589–3602, 2014.

[10] Y. Lu, Y. Cao, Q. Jin, Y. Chen, Q. Yin, J. Li, R. Zhu, and W. Zhao, "Adaboost-based detection and segmentation of bioresorbable vascular scaffolds struts in IVOCT images," in *Proc. IEEE Int. Conf. Image Process. (ICIP)*, Sep. 2017, pp. 4432–4436.

[11] C. Huang, C. Wang, J. Tong, L. Zhang, F. Chen, and Y. Hao, "Automatic quantitative analysis of bioresorbable vascular scaffold struts in optical coherence tomography images using region growing," *J. Med. Imag. Health Inform.*, vol. 8, no. 1, pp. 98–104, 2018.

[12] K. He, X. Zhang, S. Ren, and J. Sun, "Spatial pyramid pooling in deep convolutional networks for visual recognition," *IEEE Trans. Pattern Anal. Mach. Intell.*, vol. 37, no. 9, pp. 1904–1916, Sep. 2015.

[13] R. Girshick, "Fast R-CNN," in *Proc. IEEE Int. Conf. Comput. Vis. (ICCV)*, Dec. 2015, pp. 1440–1448.

[14] S. Ren, K. He, R. Girshick, and J. Sun, "Faster R-CNN: Towards real-time object detection with region proposal networks," in *Proc. Adv. Neural Inf. Process. Syst.*, 2015, pp. 91–99.

[15] Y. Cao, Q. Jin, Y. Lu, J. Jing, Y. Chen, Q. Yin, X. Qin, J. Li, R. Zhu, and W. Zhao, "Automatic analysis of bioresorbable vascular scaffolds in intravascular optical coherence tomography images," *Biomed. Opt. Express*, vol. 9, no. 6, pp. 2495–2510, 2018.

[16] O. Ronneberger, P. Fischer, and T. Brox, "U-Net: Convolutional networks for biomedical image segmentation," in *Proc. Int. Conf. Med. Image Comput. Comput.-Assist. Intervent.*, Nov. 2015, pp. 234–241.

WEN ZHOU (M'18) received the Ph.D. degree from the School of Software Engineering, Tongji University, in 2018. Since 2018, he has been with the School of Computer and Information, Anhui Normal University, Wuhu, China, where he is currently a Lecturer. He is also a member of the Chinese Computer Federation (CCF) and the Chinese Association for Artificial Intelligence (CAAI). His research interests include medical image analysis, WebVR visualization, virtual reality, and machine learning.

FEI CHEN received the M.D. and Ph.D. degrees from the Medical College, Zhejiang University, China. He is currently a Fellow Doctor with Tong Hospital, Tongji University, Shanghai. His research interests include pathophysiological proceeding of atherosclerosis, interventional treatment of CHD, image reconstruction of coronary stent, and three-dimensional (3D) visualization of coronary stent.

YONGSHUO ZONG is currently pursuing the B.Sc. degree with Tongji University, Shanghai, China. His research interests include image processing, reconstruction, and three-dimensional visualization.

DADONG ZHAO received the Ph.D. degree in computer science from Pai Chai University, South Korea, in 2014. Since 2014, he has been with the School of Computer and Information, Anhui Normal University, Wuhu, China, where he is currently a Lecturer. His research interests include machine learning and the Internet of Things.

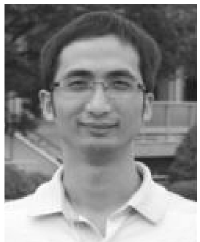

BIAO JIE received the Ph.D. degree in computer science from the Nanjing University of Aeronautics and Astronautics, China, in 2015. He joined the School of Computer and Information, Anhui Normal University, in 2006, where he is currently a Professor. His research interests include machine learning and medical image analysis.

ZHENGDONG WANG received the B.Sc. degree in computer science from the Anhui Normal University, China, in 2015, where he is currently pursuing the M.S. degree in computer science. His research interests include machine learning and medical image analysis.

CHENXI HUANG received the B.Sc. degree in computer science from Tongji University, Shanghai, China, in 2015, where he is currently pursuing the Ph.D. degree in computer science. His research interests include image processing, image reconstruction, data fusion, three-dimensional visualization, and machine learning. Since 2019, he has been the Associate Editor-in-Chief of the *Journal of Medical Imaging and Health Informatics*.

EDDIE Y. K. NG received the Ph.D. degree from Cambridge University. He is currently a Faculty Member with the College of Engineering, Nanyang Technological University, Singapore. His current research interests include thermal imaging, human physiology, biomedical engineering, computational fluid dynamics, and numerical heat transfer. He is a Fellow of the American Society of Mechanical Engineers (ASME). He received the Cambridge Commonwealth Scholarship for his Ph.D. degree. He has been the Lead Editor-in-Chief of the *Journal of Mechanics in Medicine and Biology*, since 2000. He is also the Founding Editor-in-Chief of the *Journal of Medical Imaging and Health Informatics* and an Associate Editor or an EAB of various referred international journals, such as *Artificial Intelligence*, *BioMedical Engineering OnLine*, and the *Journal of Advanced Thermal Science Research*.